Sufficient conditions for a period increment big bang bifurcation in one-dimensional maps*

Viktor Avrutin, Albert Granados   Michael Schanz†

August 11, 2010

Abstract

Typically, big bang bifurcation occurs for one (or higher)-dimensional piecewise-defined systems whenever two border collision bifurcation curves collide transversely in the parameter space. At that point, two (feasible) fixed points collide with the boundary in state space and become virtual. Depending on the properties of the map at the colliding fixed points, there exist different scenarios regarding how the infinite periodic orbits are born, mainly the so-called period adding and period increment. In our work we prove that, in order to undergo a big bang bifurcation of the period increment type, it is sufficient for a one-dimensional map to be contractive near the boundary and to have slopes of opposite sign at each side of the discontinuity.

Kewywords: organizing centers, piecewise-smooth maps, border collision bifurcations

1 Introduction

Big bang bifurcations have been reported in the literature (see references below) as a specific type of organizing centers in parameter space, where an infinite number of bifurcation curves separating existence regions of different periodic orbits issue from. Typically, this phenomenon has been detected in one-dimensional piecewise-smooth maps when globally investigating two-dimensional parameter spaces ([4, 5, 6]), although it is known that they occur also in higher-dimensional maps and flows.

---

†IPVS, University of Stuttgart, Stuttgart, Germany

The importance of these points remains on the fact that they organize the dynamics in the parameter space, as all the possible periodic orbits existing in a neighborhood of such a point are "created" there. In the cited works it was shown that the global structure of a multi-dimensional parameter space can be explained by describing only a few of such points, as the regions originating from them cover large parts of the parameter space. It was also shown that there are several types of big bang bifurcations, which cause different bifurcation scenarios to occur around them.

Usually, these detections have been performed numerically and supported by analytical calculations, as no systematic procedures in that direction have been reported until now. As these bifurcations were observed in many systems in several fields, the question arises how to predict their occurrence and how to determine their type. The goal of our work is to prove sufficient conditions for one specific type of these bifurcations.

First references of such a point were reported for a low-dimensional system in [7] when analyzing a one-dimensional two-parameter first return map of an n-dimensional flow ($n \geq 3$) near a double homoclinic connection. The homoclinic orbits are contained in a two-branched manifold and the two parameters control the overlapping between both branches. This was done for the contractive case, for which the eigenvalue corresponding to the stable direction is greater in modulus than the negative one, without distinguishing between the so-called "figure of eight" and "butterfly" configurations[1]. It is given in that reference a first scheme of the behavior of the system in the two-dimensional parameter space. The authors mentioned in a footnote that going through a certain region in this space one could find an infinite number of periodic (and also aperiodic) orbits and that this region shrinks infinitely to the origin of the parameter space, the big bang bifurcation. As in the contractive modification (see for example [19]) of the famous expansive Lorenz system, varying both parameters through that point one has that two periodic orbits in the two-branched manifold are "glued" in a double homoclinic connection. After that, infinitely many different (stable) periodic orbits looping around both branches are possible, posessing an arbitrary large number of loops before closing[2]. One month later, it was stated in [10] a first relation between the order of the loops and the Farey

---

[1]There exists a large number of publications explaining the topological differences between these two configurations. However, we refer to [13] for a compact and extensive overview.

[2]In the original expansive flow, the so-called homoclinic explosion takes place at this point [22].

numbers, and was finally proved in [11] for a contraction ratio less than $\frac{1}{2}$ and later in [9] for the pure contracting case.

Obviously, this behavior is reflected in the dynamics of the map, which is in fact our focus of interest. In general, this map has a single discontinuity at $x = 0$, and the two parameters control the gap at the discontinuity representing the overlap between both branches (see [22] for all the details). Varying these two parameters through the origin as described above, two stable fixed points (one at each side of $x = 0$) get closer until they collide at $x = 0$ at the origin of the parameter space. At that point, the map becomes continuous and, after that, the gap changes its sign and the fixed points "disappear" (become *virtual*). Then, an infinite number of (stable) different periodic orbits stepping between each side of $x = 0$ are possible.

In the context of non-smooth dynamics the previous situation is a particular case of a more general problem. Consider an n-dimensional space X split into two parts, X_ℓ and X_r, by a hypersurface Σ and two one-parameter diffeomorphisms $f_\ell(x; c_\ell), f_r(x; cr) : X \rightarrow X$. Suppose that $f_i, i \in \{\ell, r\}$, possesses a unique[3] ω-limit set given by a (stable) fixed point x_i^* and such that $x_i^* \in X_i$ if $c_i < 0$. Suppose that x_i^* crosses Σ transversely for $c_i = 0$ and consider the piecewise-defined map

$$f(x) = \begin{cases} f_\ell(x; c_\ell), & \text{if } x \in X_\ell \\ f_r(x; c_r), & \text{if } x \in X_r \end{cases}$$

It is clear that, whenever one of these points crosses transversely the boundary, f undergoes a border collision bifurcation and the fixed point becomes virtual. Then, all initial values tend to the other fixed point or, eventually, to a two-periodic orbit with one iteration at each side of Σ. However, if both fixed points become virtual (varying both parameters through $(c_\ell, c_r) = (0, 0)$) then stable periodic orbits with several iterations at each side of Σ before closing are possible. If one then encodes the periodic orbits depending on which side of Σ the consecutive iterates belong to, it is easy to see that the possible encodings of the periodic orbits mainly depend on the sign of the eigenvalues of the Jacobian matrix corresponding to the eigendirections pointing to Σ. An explicit description of which encodings are possible and which are not, for every case, remains an open problem. However, in our work we will stick to a one-dimensional map f contractive on both sides. In that case, one has $X = \mathbb{R}$, $\Sigma = \{0\}$ (up to translation)

_____

[3]We consider it unique for simplicity. Obviously, everything in what follows remains the same if both fixed points can be isolated from other ω-limit sets in a certain neighborhood.

and f becomes a map with a single discontinuity at $x = 0$. The distance between the fixed points and the boundary is controlled by the offsets at the origin, and the sign of the eigenvalues is, obviously, given by the slopes of f_ℓ and f_r near $x = 0$. Then, one can consider two different interesting cases: increasing-increasing and increasing-decreasing[4]. These two cases correspond to the first return map of the double homoclinic connection for the "butterfly" configuration; the difference between them is given by the fact whether the stable manifold along one of the branches is orientable or not which leads to different bifurcation scenarios in the $c_\ell \times c_r$ parameter space (see also [13] for a comprehensive extension of what immediately follows).

The bifurcation scenario for the increasing-increasing case was first described in [18] for a piecewise-linear map using explicit computations (see [20] for a translation). Twenty years after that, it was stated for f_ℓ and f_r quadratic maps at the same time in [12] and [23], and then studied in more detail in [19, 21] using direct computations for low periods and renormalization techniques. There, it was shown that the infinite number of periodic orbits emerging from the origin of the parameter space are created by "gluing" them and adding their periods. More recent studies ([4, 5, 6]) have shown, using direct computations and numerical simulations, that this phenomenon seems to appear for other piecewise-defined maps without any relation to the double homoclinic bifurcation. In these works this codimension-2 bifurcation was denoted as *period adding* big bang bifurcation.
On the other hand, very rigorous works ([1, 2, 3, 14, 15, 16, 17]) also gave classification, properties and the sets of periods of the possible periodic orbits using kneading invariants. This was done for expansive increasing-increasing maps (also called Lorenz-like maps) for which an explicit list of the possible periodic orbits is still missing.

The periodic orbits emerging from the origin of the parameter space for the increasing-decreasing case were first studied also in [18] for a piecewise-linear map. The resulting bifurcation scenario was proven in [13] for f_ℓ and f_r quadratic functions by collapsing the three-dimensional flow of the contractive modification of the Lorenz flow mentioned above to a 2-dimensional branched template. This bifurcation scenario was named in [4] *period increment* scenario when analyzing a piecewise-linear map, as the periods of the periodic orbits emerging at the origin of the parameter space are in-

---

[4]Recall that we are dealing in that work with maps contractive on both sides. Then, the decreasing-increasing case is equivalent to the increasing-decreasing one, and for the decreasing-decreasing one, only a two-periodic orbit or one or two fixed points are possible.

cremented by a constant value. This is precisely what we topologically independently prove in our work through Theorem 2. There we show for a *general piecewise-smooth one-dimensional map* that, whenever two (stable) fixed points collide at the boundary in such a way that the map is increasing and decreasing at each side of the discontinuity, then a big bang bifurcation of the period increment type takes place.

Although we assume for the increasing-increasing case the existence of a period adding big bang bifurcation in section 5, we emphasize that a similar rigorous result for this case has not been stated (neither proved) anywhere.

This work is organized as follows. In §2 we state some notation and definitions and present our result. In §3 we prove this result for globally contracting maps. After that, this result is extended to locally contracting ones near the discontinuity in §4. This can be proved directly but, for clarity reasons, we prefer to do this intermediate step. In order to give details on how the bifurcations occur, we obtain in §4.1 a first order approximation of the border collision bifurcation curves that emerge at the big bang bifurcation. As these two sections are mainly technical, we encourage the reader not interested on the proofs to skip them up to §5. There, by two examples, we verify the predictions and give evidences that the sufficient conditions that we use can be relaxed permitting also the slopes to vary with the parameters that control the offsets. We also verify the increasing-increasing case, and we conjecture that, in those examples, the period adding big bifurcation is caused by an infinite chain of big bang bifurcations of the period increment type. We finally conclude in §6 with some remarks.

2 Definitions, properties and statement of the results

Before restricting ourselves to the class of maps we are interested in, let us start with some standard definitions and properties of the symbolic dynamics which we are going to use in this work.

Definition 1. *Given a map $f : \mathbb{R} \to \mathbb{R}$ and $x \in \mathbb{R}$, we define the* symbolic representation of an orbit *starting at x, also called the* itinerary *of x, as $I_f(x) \in \{\mathcal{L}, \mathcal{R}\}^{\mathbb{N}}$, where*

$$I_f(x)(i) = \begin{cases} \mathcal{L} \text{ if } f^i(x) \leq 0 \\ \mathcal{R} \text{ if } f^i(x) > 0 \end{cases}, \ i \geq 0.$$

5

Definition 2. *If x belongs to a n-periodic orbit of a map f, then we will write $I_f(x) = \underline{\theta} := (\theta, \theta, \dots)$ for some finite sequence θ of length n consisting of symbols $\mathcal{L}$ and $\mathcal{R}$.*

Definition 3. *Given the shift map σ defined as $\sigma(\alpha_1, \alpha_2, \alpha_3, \dots) = (\alpha_2, \alpha_3, \dots)$ where $\alpha_i \in \{\mathcal{L}, \mathcal{R}\}$, we will say that two n-periodic sequences, $\underline{\theta_1}$ and $\underline{\theta_2}$, are shift-equivalent (or just equivalent), $\underline{\theta_1} \sim \underline{\theta_2}$, if, and only if, there exists $0 \le m < n$ such that $\sigma^m(\underline{\theta_1}) = \underline{\theta_2}$.*

It is easy to see that the relation $\sim$ defines an equivalence class in the set of symbolic sequences.

Definition 4. *We will say that a n-periodic orbit $x_1, \dots, x_n$ of a map f is of type $\underline{\theta}$ if one has $I_f(x_i) \sim \underline{\theta}$, with $1 \le i \le n$ and θ a finite sequence of length n. We will also call it a θ periodic orbit.*

Let us now consider a two-parametric map $f(x; c_\ell, c_r)$[5] of the form

$$f(x; c_\ell, c_r) = \begin{cases} c_\ell + g_\ell(x) =: f_\ell(x; c_\ell) & \text{if } x \le 0 \\ -c_r + g_r(x) =: f_r(x; c_r) & \text{if } x > 0 \end{cases} \tag{1}$$

such that

C.1 g_ℓ and g_r are smooth functions at $x = 0$ such that $g_\ell(0) = g_r(0) = 0$

C.2 There exists $\varepsilon_\ell > 0$ such that $0 \le g'_\ell(x) < 1 \ \forall x \in (-\varepsilon_\ell, 0]$

C.3 There exists $\varepsilon_r > 0$ such that $-1 < g'_\ell(x) \le 0 \ \forall x \in [0, \varepsilon_r)$

Note that if $c_\ell \ne -c_r$ then f has a discontinuity at $x = 0$. Note also that if $-1 \ll c_\ell, c_r < 0$ then the map has two fixed points, one at every side of $x = 0$ (see Fig. 1). Due to $C.2$ and $C.3$, both fixed points are attracting and, therefore, all orbits with sufficiently small initial conditions will be attracted to one of them, depending on the sign of the initial condition. If one of both parameters becomes positive, the corresponding fixed point disappears (becomes virtual trough a border collision bifurcation) and all those orbits will be attracted to the other fixed point. However, if both parameters are positive but small enough, both fixed points disappear (are virtual) and the orbits starting near the origin stay forever near the origin jumping from one side of $x = 0$ to the other one. The possible asymptotic behaviors of these orbits is precisely what our result describes, which is reflected in the next

---

[5]We will also avoid writing the dependence on the parameters explicitly and we will refer to it just as $f(x)$ or f.
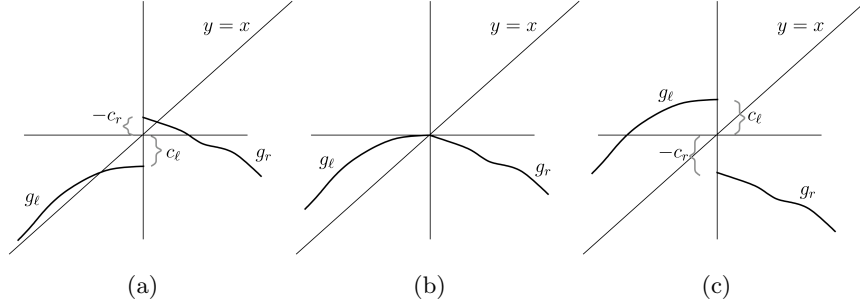
Figure 1: Influence of the parameters c_ℓ, c_r on a map as defined in (1). a) $c_\ell, c_r < 0$, b) $c_\ell = c_r = 0$ and c) $c_\ell, c_r > 0$.

Theorem 1. *Let f be a map of type (1) fulfilling conditions C.1–C.3. Then, there exists $\varepsilon_0 > 0$ such that, for every $n > 0$ arbitrary large and every $\varepsilon_0 > \varepsilon > 0$,*

a) *There exist two curves[6] in parameter space $c_\ell \times c_r$, $\xi^d_{\mathcal{RL}^{n-1}}(c_\ell)$ and $\xi^c_{\mathcal{RL}^{n+1}}(c_\ell)$, passing through the origin, such that for every $0 < c_\ell < \varepsilon$ with $\xi^d_{\mathcal{RL}^{n-1}}(c_\ell) < c_r < \xi^c_{\mathcal{RL}^{n+1}}(c_\ell)$, there exists a unique periodic orbit, which is stable and of type $\underline{\mathcal{RL}^n}$.*

b) *For every $0 < c_\ell < \varepsilon$, $\xi^c_{\mathcal{RL}^{n+1}}(c_\ell) < c_r < \xi^d_{\mathcal{RL}^n}(c_\ell)$, there coexist two periodic orbits, which are stable and of type $\underline{\mathcal{RL}^n}$ and $\underline{\mathcal{RL}^{n+1}}$.*

Moreover, for $(c_\ell, c_r) = (0, 0)$ there exists an open set containing the origin where the unique invariant object is the stable fixed point $x = 0$.

This means that, when considering the parameter space $c_\ell \times c_r \simeq \mathbb{R}^2$, there exists an infinite number of border collision bifurcation curves emerging from the origin, $\xi^{d,c}_{\mathcal{RL}^n}$, separating all the possible dynamics that one can find near $x = 0$. These curves are ordered anti-clockwise as follows (see also Fig 7(a) for a graphical explanation). Given $n \geq 1$, one first finds a curve where an $\underline{\mathcal{RL}^n}$ periodic orbit is created through a border collision, $\xi^c_{\mathcal{RL}^n}$, and coexists with an other one of type $\underline{\mathcal{RL}^{n-1}}$ until one finds the curve $\xi^d_{\mathcal{RL}^{n-1}}$ where the $\underline{\mathcal{RL}^{n-1}}$ orbit is destroyed. After that, only the $\underline{\mathcal{RL}^n}$ periodic orbit exists until the next border collision bifurcation occurs at the curve

---

[6]The meaning of the upper indices d and c refer to "creation" and "destruction" of the corresponding periodic orbits.

$\xi^c_{\mathcal{RL}^{n+1}}$ where a periodic orbit of type $\underline{\mathcal{RL}^{n+1}}$ is created. Again, both orbits coexist until the $\underline{\mathcal{RL}^n}$ periodic orbit is destroyed at $\xi^d_{\mathcal{RL}^n}$. This procedure is repeated ad infinitum, starting with the curve $\xi^c_{\mathcal{RL}}$ which is located in the 4th quadrant and continuing with ξ^d_R which is the horizontal axis. All other border collision bifurcation curves mentioned above are located in the first quadrant and accumulate at the vertical axis. Details on how these bifurcation curves are obtained will be given in §4.1. As already stated in Theorem 1, all the dynamics described above disappear at the origin of the parameter space, where only a stable fixed point exists.

Regarding what has been said in the introduction, we will refer to such a point as a *Big Bang* bifurcation. In particular, for the situation exposed above one has the following

Definition 5. *Let B be a point in a 2-dimensional parameter space such that the bifurcation scenario along the boundary of an arbitrary small neighborhood of B is equivalent to the one exposed in Theorem 1 for the origin. Then we will say that there exists a big bang bifurcation of period increment type in B.*

Then one can formulate Theorem 1 in a more compact form as

Theorem 2. *For a map of type (1) which satisfies the conditions C.1–C.3, the origin of the parameter space $c_r \times c_\ell$ represents a big bang bifurcation point of the period increment type.*

3   Increasing-decreasing globally-contracting maps

As already mentioned in the introduction, in this section we will harden conditions C.1–C.3 to be globally fulfilled and prove our main result in this case. Then, in §4 using a simple result (Lemma 8) we will see that Theorem 2 also holds for conditions C.1–C.3.
Before going into details, let us state the strategy that we are going to follow. In order to show that only $\underline{\mathcal{RL}^n}$ periodic orbits are possible for $c_\ell, c_r > 0$, we will show that other type of periodic orbits can not exist (Lemmas 1, 2, 3 and 6). Then, considering the sequence of preimages of 0 by f_ℓ, we will see that $\underline{\mathcal{RL}^n}$ periodic orbits exist for every n (Lemma 7), that they are created and destroyed via border collision bifurcations and that at most two of them can coexist (Lemma 5).

Let us consider a map of the form defined in (1) such that

C.1' $g_\ell(x)$ and $g_r(x)$ are smooth functions such that $g_r(0) = g_\ell(0) = 0$

C.2' $0 \le g'_\ell(x) < 1$ if $x \le 0$

C.3' $-1 < g'_r(x) \le 0$ if $x \ge 0$

C.4' f is unbounded.

We start proofs of these results with the next

Lemma 1. *Given $\theta = I_f(x)$ with f as defined in (1) fulfilling the conditions C.1'–C.4', if $I_f(x)(i) = \mathcal{R}$ and $c_r > 0$ then $I_f(x)(i+1) = \mathcal{L}$. That is, no consecutive $\mathcal{R}$'s are possible in θ.*

Proof. Obvious, as $(0, \infty)$ is mapped into $(-\infty, 0)$. $\qquad\square$

Remark 1. *Note that the previous Lemma does not need $I_f(x)$ to be a periodic sequence.*

Lemma 1 obviously prohibits $\underline{\mathcal{R}^n}$ periodic orbits to exist. Although two consecutives $\mathcal{L}$'s are possible, $\underline{\mathcal{L}^n}$ periodic orbits are not, as the next result shows.

Lemma 2. *If x belongs to a periodic orbit of a map f as defined in (1) fulfilling the conditions C.1'–C.4', then, if $c_\ell > 0$ there exists an i such that $I_f(x)(i) = \mathcal{R}$.*

Proof. If $x > 0$, then one has $I_f(x)(0) = \mathcal{R}$. Otherwise, as f_ℓ is monotonically increasing with slope less than one and $f_\ell(0) > 0$, further iterates of x by f_ℓ will necessarily reach the positive domain. $\qquad\square$

As a next step we show now that the word $\mathcal{RL}^n\mathcal{RL}^n$ can not be contained in any periodic orbit. It is worth to emphasize that with such a word, we obviously refer here (and in the following) to the compact representation, that is, it has to be followed by an $\mathcal{R}$, because a successive $\mathcal{L}$ would lead to the word $\mathcal{RL}^n\mathcal{RL}^{n+1}$. This result is shown in the next Lemma based on a similar one presented in [13]. It is stated there using geometrical arguments in the Lorenz template that similar orbits are not possible for a three-dimensional flow undergoing a homoclinic bifurcation of the single twisted butterfly type. By contrast, we will use here only the nature of the map to prove it.
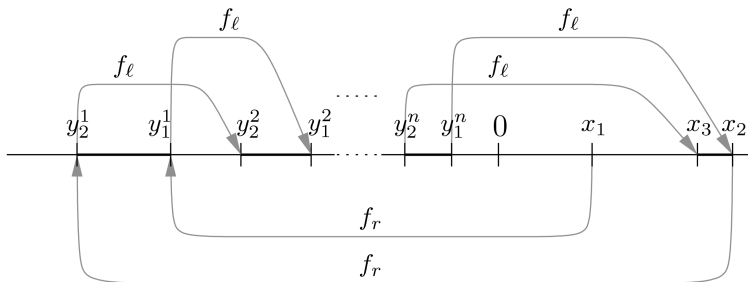
Figure 2: "Trapped" orbit

Lemma 3. *If f is of type (1) with $c_\ell, c_r > 0$, holding C.1'–C.4', and there exists x_1 such that $I_f(x_1) = \underline{\theta}$, then the word $\mathcal{RL}^n\mathcal{RL}^n$ can not be contained in θ.*

Proof. Let us suppose that there exists x_1 such that $I_f(x_1) = \underline{\theta}$ with $\theta = \mathcal{RL}^n\mathcal{RL}^n\theta_2$ for some finite word θ_2. Note that using the relation $\sim$ one can consider that θ is given in this form. Let us write this periodic orbit as

$$\underbrace{x_1, y_1^1, y_1^2, \ldots, y_1^n, x_2, y_2^1, y_2^2, \ldots, y_2^n}_{\mathcal{RL}^n\mathcal{RL}^n}, \underbrace{x_3, \ldots,}_{\theta_2} \underbrace{x_1, \ldots}_{\mathcal{RL}^n\mathcal{RL}^n}, \ldots,$$

where $x_i > 0$ and $y_i^j < 0$ (see Fig. 2). Let us also assume that $x_1 < x_2$ (otherwise the same argument can be performed with the points x_2 and x_3) and let us iterate the whole interval $[x_1, x_2]$. As f_r is decreasing and $c_r > 0$, $f_r([x_1, x_2]) = [y_2^1, y_1^1]$ with $f_r(x_2) = y_2^1 < f_r(x_1) = y_1^1 < 0$, the interval is twisted. Moreover, as f_r and f_ℓ are, respectively, decreasing and increasing contracting functions, we have

$$\mu([x_1, x_2]) > \mu([y_2^1, y_1^1]) > \mu([y_2^2, y_1^2]) > \cdots > \mu([y_2^n, y_1^n]) > \mu([x_3, x_2]),$$

where $\mu([a, b]) = |b - a|$ is the length of the interval $[a, b]$.

Now, as f_ℓ preserves orientation and the length of $[x_1, x_2]$ is decreased, $x_3 \in (x_1, x_2)$ and therefore $y_3^1 = f_r(x_3)$ needs also n iterations to return to the right side.

Repeating the same argument with $[x_3, x_2]$, one has that $f_l^n(y_3^1) = x_4 \in (x_3, x_2)$. Iterating the argument, the orbit of x_1 will be "trapped" in (x_3, x_2) and will never reach x_1 again, so it can not be periodic. $\qquad\square$

Remark 2. *Note that it is crucial in the last proof that both points x_1 and x_2 return to the right domain $(0, \infty)$ after exactly the same number n of*

10

iterations by f_ℓ. That is, the interval $f^m([x_1, x_2])$ remains connected for all m.

Before considering periodic sequences containing the word $\mathcal{RL}^n\mathcal{RL}^m$ with $n \neq m$, let us state some properties and definitions of maps of type (1) fulfilling the conditions C.1'–C.4'.

We first note that the left branch f_ℓ reaches its maximum value at $x = 0$ ($f_\ell(0) = c_\ell > 0$) and, therefore, when a point $y < 0$ is re-injected into the right domain by f_ℓ it has to be necessarily in $(0, c_\ell]$. On the other hand, as f_r is monotonically decreasing, every point $x \in (0, c_\ell]$ will be injected into the left domain in the interval $[\nu, 0]$, where $\nu = f_r(c_\ell) < 0$. Hence, the interval $[\nu, c_\ell]$ acts as an "absorbing" interval as all orbits starting at any point $x \in \mathbb{R}$ will reach it after some number of iterations and will never leave it. Therefore we have the next

Lemma 4. *Let $f(x)$ be a map of type (1) which fulfills the conditions C.1'–C.4' and let $\nu = f_r(c_\ell)$. For every $x \in \mathbb{R}$ there exists an m_0 such that $f^m(x) \in [\nu, c_\ell] \ \forall m \geq m_0$. Therefore, the map f can be considered as a map on the interval $[\nu, c_\ell]$:*

$$f : [\nu, c_\ell] \to [\nu, c_\ell]$$

Remark 3. *Note that this global reduction is true as functions g_ℓ and g_r are globally increasing and contractive (C.1'–C.4'). In the next section, where the conditions C.1'–C.4' are going to be relaxed, this reduction will be valid only locally.*

Let us now consider the sequences $\{a_n\}$ and $\{b_n\}$ formed, respectively, by the preimages of 0 by the left branch and by the preimages of these preimages by the right branch

$$a_0 = 0, \quad a_n = f_\ell^{-1}(a_{n-1}) \text{ with } n > 0, \tag{2}$$

$$b_n = f_r^{-1}(a_n) \text{ with } n \geq n_0, \tag{3}$$

with some n_0 as explained below (see Fig. 3). Note that, as f_ℓ is a monotonically increasing function, if $c_\ell > 0$ the sequence $\{a_n\}$ verifies $a_{n+1} < a_n \leq 0$ $\forall n \geq 0$[7]. Although the preimages of 0 by the left branch (a_n) exist $\forall n$, b_n is defined for $n \geq n_0$ where n_0 is such that $a_{n_0} \leq -c_r < a_{n_0-1}$.

Due to the contractiveness of both functions f_ℓ and f_r, the following in-

------

[7]Note that $f^0(0) = 0$ as the function $f^0(x)$ equals the identity.

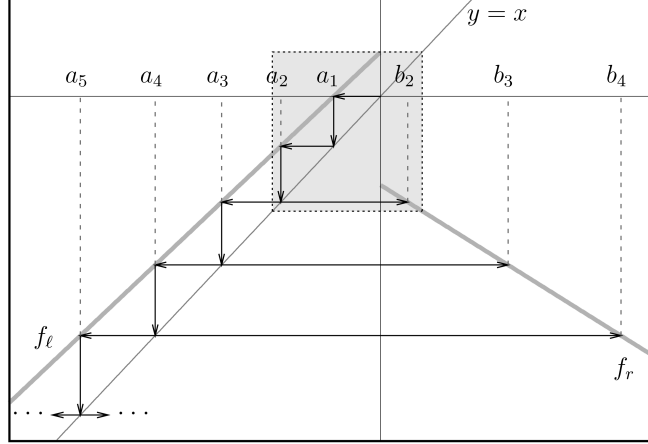Figure 3: Definition of the sequences $\{a_n\}$ and $\{b_n\}$. The box shown dotted corresponds to the absorbing interval.

equalities hold

$$\frac{\mu([a_{n+1}, a_n])}{\mu([a_n, a_{n-1}])} > 1, \ n > 0 \tag{4}$$

$$\frac{\mu([b_n, b_{n+1}])}{\mu([b_{n-1}, b_n])} > 1, \ n > n_0.$$

The sequence $\{a_n\}$ defined in Eq. (2) splits the interval $(-\infty, 0]$ into sub-intervals of the form $(a_{n+1}, a_n]$ (see Fig. 3) such that $\forall y \in (a_{n+1}, a_n]$ the number of iterations needed by y to return to the right domain is exactly $n + 1$. On the other hand, the intervals $(0, b_{n_0})$ and $[b_n, b_{n+1})$ with $n \geq n_0$, form a partition of $(0, \infty)$, such that $\forall x \in [b_n, b_{n+1})$ the point $f_r(x)$ needs exactly $n + 1$ iterations by f_ℓ to return to the positive domain.

For a fixed value $(c_\ell, c_r) \in \mathbb{R}^+ \times \mathbb{R}^+$, the number of iterations that a periodic orbit can perform in the negative domain is determined by the number of elements of the sequence $\{b_n\}$ contained in the absorbing interval $[\nu, c_\ell]$. For example if b_2 and b_3 would be contained in the absorbing interval $[\nu, c_l]$, then the number of iterations of a periodic orbit can be two, three or four. However, as the next result shows, at most one element of the sequence $\{b_n\}$ can be contained in the absorbing interval $[\nu, c_\ell]$.
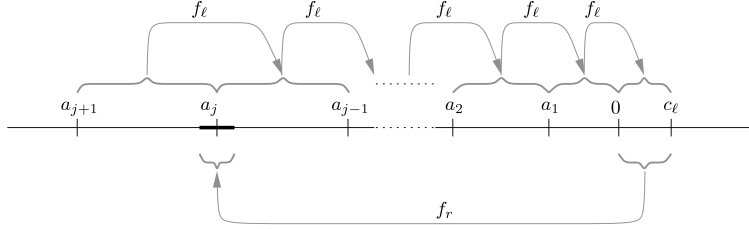
Figure 4: Backward and forward iterates of $(0, c_\ell]$. $f_r((0, c_\ell])$ (dark segment) is smaller than $f_\ell^{-n}((0, c_\ell])$ $\forall n$. Therefore, at most one a_j can be reached by $f_r((0, c_\ell])$.

Lemma 5. *If f is a map of type (1) fulfilling conditions C.1'–C.4', then there exists at most one a_j (equiv. b_j) such that $a_j \in f_r((0, c_\ell])$ (equiv. $b_j \in (0, c_\ell]$).*

Proof. Recalling that $c_\ell = f_\ell(0)$, one has (see Fig. 4)

$$[a_{n+1}, a_n] = f_\ell^{-1}([a_n, a_{n-1}])$$
$$[a_1, 0] = f_\ell^{-1}([0, c_\ell]).$$

Using the property shown in Eq. (4) one has

$$\mu([0, c_\ell]) < \mu([a_{n+1}, a_n]) \ \forall n,$$

and, since f_r is a contractive function one obtains

$$\mu(f_r((0, c_\ell])) < \mu([a_{n+1}, a_n]) \ \forall n.$$

Therefore, at most one a_n can be located in $f((0, c_\ell])$. $\qquad\square$

For a fixed j, the uniqueness of such a b_j (in case of existence) in the last Lemma implies that the periodic sequences of a map under the considered conditions can be either $\underline{\mathcal{RL}^j}$, $\underline{\mathcal{RL}^{j+1}}$ or sequences containing these two words only. However, what we want to show is that the last case is not possible and in fact the only admissible periodic sequences are exactly $\underline{\mathcal{RL}^j}$ and $\underline{\mathcal{RL}^{j+1}}$. Therefore, let us consider the two only possible cases: for a certain j, either $(0, c_\ell] \subset (b_j, b_{j+1})$ (which means $b_j = 0$ or $b_j \notin [0, c_\ell]$) or $(0, c_\ell] = (0, b_j) \cup [b_j, c_\ell]$ (which means $b_j \in (0, c_\ell]$) $(c_\ell < b_{j+1})$, which is the case shown in Fig. 3.

In the first case, as the periodic orbits have to be contained in the interval

13

$[\nu, c_\ell]$, they always need the same number of iterations on the negative domain and the result comes from Lemmas 1, 2 and 3.

In the second case, we have to show that if a periodic orbit reaches $(0, b_j)$ it can not reach $[b_j, c_\ell]$ and vice versa, that is, once an orbit enters the absorbing interval $[\nu, c_\ell]$, the number of iterations needed to return to the positive domain is preserved and is either j or $j + 1$.

Both cases are included in the following

Lemma 6. *Let f be a map as defined in (1) fulfilling conditions C.1'–C.4'. If $x \in \mathbb{R}$ belongs to a periodic orbit of f then there exists $n > 0$ such that $I_f(x) = \underline{\mathcal{R}\mathcal{L}^n}$ up to shift-equivalence.*
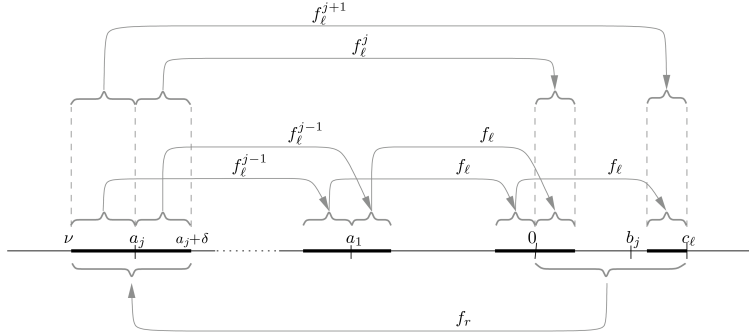

Figure 5: The interval $f_r((0, c_\ell])$ is split at its return to the right domain.

Proof. If $\nexists\, a_j \in f_r((0, c_\ell])$, then the result comes from Lemmas 1, 2 and 3. Now let us suppose that there exists $a_j \in f_r((0, c_\ell])$ which, by Lemma 5, must be unique. We also have a unique $b_j \in (0, c_\ell]$. As f_r is monotonously decreasing and thus the interval $(0, c_\ell]$ is inverted, we can write

$$f_r((0, c_\ell]) = [\nu, a_j + \delta)$$

for some $\delta > 0$.

As f_ℓ is continuous in $(-\infty, 0]$ and $f_\ell(a_n) = a_{n-1} \;\forall n > 1$, the interval $f_\ell^n([\nu, a_j + \delta))$ remains connected and contains a_{j-n} for $n = 1, \ldots, j$ (see Fig. 5). For $n = j$, the interval contains 0 and therefore it contains positive and negative points. The positive ones are immediately mapped into $(a_j, a_j + \delta)$ by f_r in such a way that $f_r(0^+) = (a_j + \delta)^-$. Negative points need one more iteration by f_ℓ and will be mapped into $(b_j, c_\ell]$ with $f_\ell(0^-) = c_\ell^-$,

14

so the initial interval is split. After that, these points will be mapped into $[\nu, a_j)$ verifying that $f_r(c_\ell^-) = \nu^+$. Summarizing,

$$f_r((0, b_j)) = (a_j, a_j + \delta)$$
$$f_r([b_j, c_\ell] = [\nu, a_j]$$

and

$$f_\ell^{j+1}([\nu, a_j]) \subset [b_j, c_\ell]$$
$$f_\ell^j((a_j, a_j + \delta)) \subset (0, b_j),$$

so

$$f_\ell^{j+1}(f_r([b_j, c_\ell])) \subset [b_j, c_\ell]$$
$$f_\ell^j(f_r(0, b_j)) \subset (0, b_j),$$

and the number of steps needed by an orbit starting in $(0, c_\ell]$ to be re-injected to the positive domain will remain constant and equal to j or $j+1$ depending on whether it starts in $(0, b_j)$ or $[b_j, c_\ell]$, respectively. Therefore, only symbolic sequences of the form $\mathcal{RL}^j\mathcal{RL}^j\ldots$ or $\mathcal{RL}^{j+1}\mathcal{RL}^{j+1}\ldots$ with starting points in $(0, c_\ell]$ are possible.

As it has been proven above, that the number of steps on the left side of a periodic orbit must be preserved, we can apply Lemma 3 to show that if x belongs to a periodic orbit of a map under the considered conditions, then necessarily $I_f(x) = \underline{\mathcal{RL}^n}$ for some $n > 0$. $\qquad\square$

Now we ask about the reciprocal of Lemma 6, that is, we want to show that periodic orbits of type $\underline{\mathcal{RL}^n}$ exist $\forall n > 0$.

Lemma 7. *Let f be of the form defined in (1) and fulfilling conditions C.1'–C.4'. Then, for every $n \geq 1$ and every $c_\ell > 0$, there exists $c_r > 0$ such that f possesses an orbit with the symbolic sequence $\underline{\mathcal{RL}^n}$.*

Proof. It is clear that for every $n \geq 2$ and every $c_\ell > 0$ there exists $c_r > 0$ such that
$$f_r((0, c_\ell]) \cap [a_n, a_{n-2}] \neq \emptyset,$$
which can be given due to one of the next three situations (see Figs. 4 and 5)

    S.1 $a_{n-1} \in f_r(0, c_\ell])$

<div align="center">15</div>

S.2 $f_r(0, c_\ell] \subset (a_n, a_{n-1})$

S.3 $a_n \in f_r((0, c_\ell])$

If S.1 holds, $b_{n-1} \in (0, c_\ell]$ and

$$f_\ell^n f_r : [b_{n-1}, c_\ell] \longrightarrow [b_{n-1}, c_\ell]$$
$$f_\ell^{n-1} f_r : (0, b_{n-1}) \longrightarrow (0, b_{n-1}),$$

are continuous contracting functions which must have a unique (stable) fixed point. Therefore, two stable periodic orbits $\underline{\mathcal{RL}^n}$ and $\underline{\mathcal{RL}^{n-1}}$ coexist. Note that for $n = 2$ this proves also the existence of a $\underline{\mathcal{RL}}$ orbit.

In the second case (S.2), $b_{n-1} \notin (0, c_\ell]$ ($[0, c_\ell] \subset (b_{n-1}, b_n)$) and

$$f_\ell^n f_r : (0, c_\ell] \longrightarrow (0, c_\ell]$$

is a continuous contracting function which also must have a unique (stable) fixed point. In this case, there exists a unique periodic orbit of type $\underline{\mathcal{RL}^n}$ which is the unique attractor in a sufficiently small vecinity of $x = 0$.

Finally, if S.3 holds, replacing n by $n - 1$ and arguing as in S.1, one has that a stable periodic orbit of type $\underline{\mathcal{RL}^n}$ coexists with a stable $\underline{\mathcal{RL}^{n+1}}$ periodic one. $\qquad \square$

Remark 4. *By contrast to all orbits $\underline{\mathcal{RL}^n}$ with $n \geq 2$, the periodic orbit $\underline{\mathcal{RL}}$ exists not only for $c_r > 0$ but also for $c_r \leq 0$. In that case, it coexists with the fixed point $\underline{\mathcal{R}}$.*

Remark 5. *Note that the transitions between cases S.1, S.2 and S.3 are given by border collision bifurcations where the respective periodic orbits are created or destroyed when they collide with the boundary $x = 0$. This defines the curves ξ^c and ξ^d used in Theorem 1. See §4.1 for more details.*

Remark 6. *As it is known, invariant objects of piecewise-smooth systems do not necessarily have to be separated by another invariant object. In this case, the coexistence of stable periodic objects may also be separated by the discontinuity (and its preimages) (see [8] for an extensive overview about piecewise-smooth dynamics).*

Theorem 3. *For a map of type (1) which fulfills the conditions C.1'–C.4', the origin of the parameter space $c_\ell \times c_r$ represents a big bang bifurcation point of the period increment type.*

16

Proof. It is clear that for $(c_\ell, c_r) = (0, 0)$ the map f possesses a stable fixed point at $x = 0$. Now we have to show that an infinite number of bifurcation curves separating existence regions of different periodic orbits are issuing from the origin. As a second step we have to show that a smooth change of the parameters across the bifurcation curve confining the regions of existence of a unique $\underline{\mathcal{RL}^n}$ orbit lead to the creation of (coexisting) $\underline{\mathcal{RL}^{n+1}}$ or $\underline{\mathcal{RL}^{n-1}}$ periodic orbits.

The key to show the first step is the fact that the sequence $\{a_n\}$ collapses to the origin as $c_\ell \to 0$, that is

$$\lim_{c_\ell \to 0} a_n = 0 \; \forall n \geq 1.$$

This is due to the continuity of f_ℓ and the fact that it is a monotonically increasing function. As $[a_1, 0] = f_\ell^{-1}([0, c_\ell])$ (compare Fig. 4), it is clear that $a_1 \to 0$ as $c_\ell \to 0$. Now, iterating the argument and using that $a_n = f_\ell^{-1}(a_{n-1})$, it is clear that for every $\varepsilon > 0$, arbitrarily small, there exists $c_\ell(\varepsilon)$ small enough such that $-\varepsilon < a_n < 0$. By Lemma 7, there exists c_r such that $f_r((0, c_\ell])$ contains a_n and, therefore, a periodic orbit of type $\underline{\mathcal{RL}^n}$ exists.

On the other hand, it is clear that $c_r \to 0$ as $a_n \to 0$ and, therefore, a $\underline{\mathcal{RL}^n}$ periodic orbit exists for every n for values of (c_ℓ, c_r) arbitrarily close to the origin. Finally, if $(c_\ell, c_r) = (0, 0)$, the map possesses a stable fixed point which absorbs all orbits and thus all periodic orbits disappear at that point. $\square$

4 Increasing-decreasing locally-contracting maps

In this section we relax the global monotonically-contracting conditions C.1'–C.4' to be fulfilled near the origin and show that the results of the previous section are valid sufficiently close to the origin of the parameter space. Thus we restrict our selves to maps of type (1) fulfilling the conditions C.1–C.3.

Due to the smoothness of functions f_ℓ and f_r near the origin, there exists an open neighborhood of this point where both functions are contracting and which contains the absorbing interval $[\nu, c_\ell]$ if c_r and c_ℓ are small enough.

On the other hand, the values of c_r given by Lemma 7 tend to 0 as $c_\ell \to 0^+$, and therefore all results of the previous section hold under these conditions. From the previous arguments one has the next result, which proves Theorem 2.

Lemma 8. *Let f be a map of type (1) keeping conditions C.1–C.3. Then there exist c_ℓ^0 and c_r^0 such that if $0 < c_\ell < c_\ell^0$ and $0 < c_r < c_r^0$ f is contracting in $[\nu, c_\ell]$. Moreover, for every $c_r < c_r^0$ and every n, there exists $0 < \varepsilon < c_\ell^0$ such that $a_j \in [\nu, 0] \ \forall j \leq n$ if $c_\ell < \varepsilon$.*

Remark 7. *If one changes condition C.3' by g_r to be a constant function for $x \geq 0$, then all the results presented above are still valid except for one detail. In such a case, one has only to take into account that, as $f_r((0, c_\ell])$ would be a single point. Then, conditions S.1 and S.3 in the proof of Lemma 7 become $a_{n-1} = f_r(0, c_\ell])$ and $a_n = f_r((0, c_\ell])$, respectively, preventing the coexistence between two different orbits. Therefore, (ii) in Theorem 1 no longer holds as $\xi_{\mathcal{RL}^{n-1}}^c = \xi_{\mathcal{RL}^n}^d$. Such a situation has been referred to in the literature ([4]) as* pure period increment *scenario, and therefore the origin of the parameter space represents a* pure period increment *big bang bifurcation.*

Recalling Remark 5, the orbits given in Theorem 2 are created and destroyed at border collision bifurcations curves, which are mentioned in the first version of the same result, Theorem 1. In the next section, approximating them up to first order, we will give details on how are they obtained.

4.1 Border collision curves near the origin

Given $n > 0$ and $c_\ell > 0$ (which we will always assume to be small enough), we know (Lemma 7) that there exists $c_r > 0$ such that one of the next cases hold

S.1 $a_{n-1} \in f_r(0, c_\ell])$

S.2 $f_r(0, c_\ell] \subset (a_n, a_{n-1})$

S.3 $a_n \in f_r((0, c_\ell])$

implying the existence of an $\underline{\mathcal{RL}^n}$ periodic orbit. As has been shown in the proof of Lemma 7, every case above leads to different dynamics. Therefore, the limiting parameter values define the (border collision) bifurcation. Then for each of the cases above, for every c_ℓ we will find the extremal value of c_r and obtain the bifurcation curves, $\xi_{\mathcal{RL}^n}^{c,d}$, mentioned in Theorem 1 at which an $\underline{\mathcal{RL}^n}$ orbit is created or destroyed.

The smallest value of c_r which leads S.1 to be fulfilled is given by

$$f_r(c_\ell) = a_{n-1} \tag{5}$$

and corresponds to the creation of the $\underline{\mathcal{RL}^n}$ periodic orbit coexisting with the $\underline{\mathcal{RL}^{n-1}}$ one.

The transition between S.1 to S.2 is given by

$$f_r(0) = a_{n-1}$$

where the periodic orbit $\underline{\mathcal{RL}^{n-1}}$ no longer exists leading $\underline{\mathcal{RL}^n}$ be the unique attractor (near the origin).

Increasing c_r, one finds the value of this parameter which satisfies the condition

$$f_r(c_\ell) = a_n.$$

At this parameter value, representing the transition from S.2 to S.3, the $\underline{\mathcal{RL}^{n+1}}$ orbit is created and coexists with $\underline{\mathcal{RL}^n}$.

Finally, the next bifurcation is given by

$$f_r(0) = a_n \tag{6}$$

where the periodic orbit $\underline{\mathcal{RL}^n}$ is destroyed as S.3 no longer holds.

Summarizing, for every $c_\ell > 0$ and $n > 0$, Eqs. (5) and (6) give the value of c_r for the border collision bifurcations where, respectively, the $\underline{\mathcal{RL}^n}$ periodic orbit is created and destroyed. Therefore, in parameter space, the respective border collision bifurcations curves in a sufficiently small open set $\mathcal{U}$ of the origin will be given by

$$\xi^c_{\mathcal{RL}^n} = \{(c_\ell, c_r) \in \mathcal{U}, \ c_\ell > 0 \mid f_r(c_\ell) = a_{n-1}\}$$
$$\xi^d_{\mathcal{RL}^n} = \{(c_\ell, c_r) \in \mathcal{U}, \ c_\ell > 0 \mid f_r(0) = a_n\}$$

Now, in order to obtain a linear approximation of these curves, let us assume that functions f_ℓ and f_r are analytic and hence we can consider their power expansions up to first order

$$f(x) = \begin{cases} f_\ell(x) = c_\ell + g'_\ell(0)x + O(x^2) & \text{if } x \leq 0 \\ f_r(x) = -c_r + g'_r(0)x + O(x^2) & \text{if } x > 0. \end{cases} \tag{7}$$

If $g'_\ell(0) > 0$, the preimages of $a_0 = 0$ by f_ℓ are given by

$$a_j = -\sum_{i=1}^{j} \frac{c_\ell}{(g'_\ell(0))^i} + O(c_\ell^2), \ j > 0. \tag{8}$$

19

Using Eq. (8) and solving Eqs. (5) and (6) one has that

$$\xi^c_{\mathcal{RL}^n} = \left\{ (c_\ell, c_r) \in \mathcal{U}, \ c_\ell > 0 \mid c_r = c_\ell \left(\sum_{i=1}^{n-1} \frac{1}{(g'_\ell(0))^i} + g'_r(0) \right) + O(c_\ell^2) \right\}$$

(9)

$$\xi^d_{\mathcal{RL}^n} = \left\{ (c_\ell, c_r) \in \mathcal{U} \mid c_r = \sum_{i=1}^{n} \frac{c_\ell}{(g'_\ell(0))^i} + O(c_\ell^2) \right\}$$

(10)

Note that, as mentioned in §2, the $\xi^c_{\mathcal{RL}}$ bifurcation curve is located in the 4th quadrant, as the sum vanishes for $n = 1$ and $g'_r(0) < 0$. All other curves are located in the first quadrant.

Obviously, one can proceed in the same way in order to have an approximation up to higher order just considering the corresponding higher order terms in Eq. (7).

5   Examples

In this section we will illustrate the results obtained so far with two examples.

5.1   Example 1

Let us consider

$$f(x) = \begin{cases} c_\ell + 0.9 \sin(x) & \text{if } x \leq 0 \\ -c_r - 0.5 \sin(x) & \text{if } x > 0 \end{cases}$$

(11)

shown in Fig. 6, which fulfills the conditions C.1–C.3.

As one can see in Fig. 7, there exists a big bang bifurcation of the period increment type at the origin of the parameter space $c_\ell \times c_r$, as predicted by Theorem 2. A global overview of the bifurcation scenario is presented in Fig. 7(a), and a blow up near the origin of this space is shown in Fig. 7(b). There one can see an infinite number of border collision bifurcation curves separating the regions of existence of the different periodic orbits. There it is also shown the first order approximation of the bifurcation curves reported in §4.1. As one can see in the one-dimensional bifurcation diagram presented in Fig. 7(c) along the curve parametrized by ϕ in Fig. 7(b), the periodic orbits that exist near the origin are of type $\underline{\mathcal{RL}^n}$. As labeled in the figures,
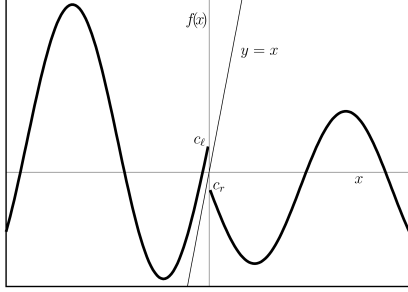
Figure 6: System function of Example 1 defined in Eq. (11)

there exist regions where only one periodic orbit of type $\underline{\mathcal{RL}^n}$ exists, and there exist other regions where two periodic orbits of type $\underline{\mathcal{RL}^n}$ and $\underline{\mathcal{RL}^{n+1}}$ coexist.

As one can see in Fig. 7(a), near $(0, \pi)$ there exists another point where an infinite number of bifurcation curves seem to emerge from.

In order to investigate this point in more detail, let us first note that it is given by the intersection between the border collision bifurcation curves $\xi_{\mathcal{R}}^d$ (the vertical axis) and $\xi_{\mathcal{RL}}^d$. This means that, at this point, a periodic orbit of type $\underline{\mathcal{RL}}$ collides with the boundary together with the fixed point $\underline{\mathcal{L}}$. This is exactly what we have considered in that work, the simultaneous collision of two fixed points with the boundary. Let us therefore consider the following composite map

$$f_2(x) = \begin{cases} f_\ell(x) & \text{if } x \leq 0 \\ f_\ell f_r(x) & \text{if } x > 0 \end{cases} \tag{12}$$

which collapses the $\underline{\mathcal{RL}}$ periodic orbit of (11) to a the fixed point $\underline{\mathcal{R}}$. Easily, one sees that, at $(c_\ell, c_r) = (0^+, \pi^-)$, $f_\ell(0) = 0^+$, $f_\ell f_r(0) = 0^-$, $f_\ell'(0^-) > 0$ and $(f_\ell f_r)'(0^+) > 0$. This means that $f_2(x)$ is continuous at the parameter values $(0, \pi)$ and positive-negative offsets appear when increasing c_ℓ and decreasing c_r. However, $f_2(x)$ does not fulfill the conditions of Theorem 2 as the map increases on each side of the discontinuity. Moreover, the slope at the origin of the right branch, $(f_\ell f_r)'(0) = -0.5 \cdot 0.9 \cos(-c_r)$, depends on the parameter c_r. However, if we consider the power series expansions of the gap and the slope of the right branch of $f_2(x)$ at $x = 0$ near $(c_\ell, c_r) = (0, \pi)$
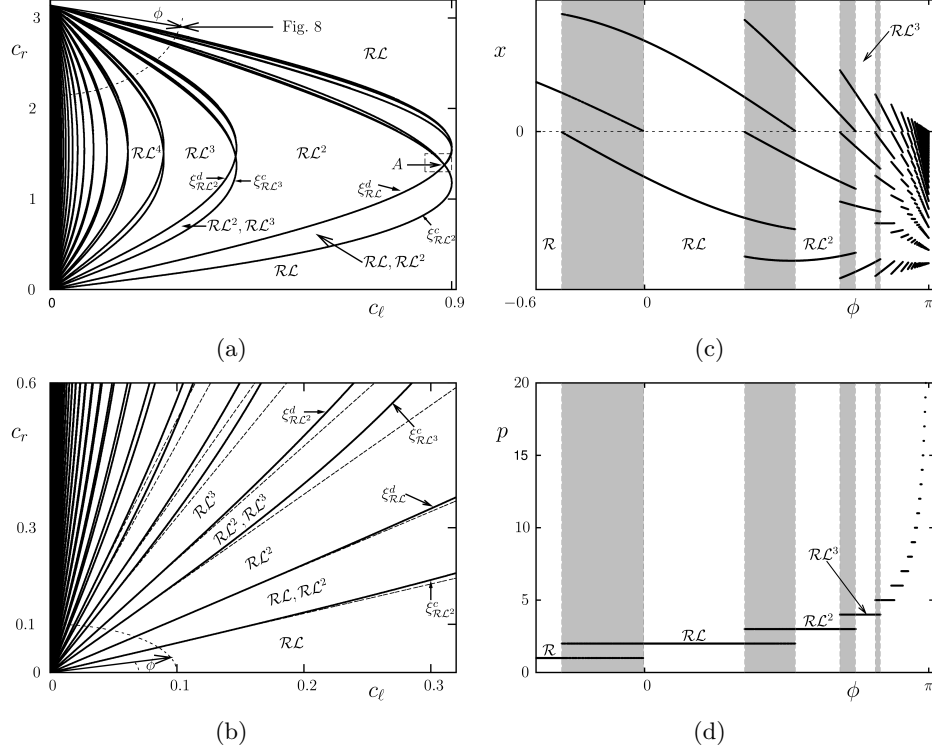
21

Figure 7: (a): border collision bifurcation curves for Example 1. A blow up of the neighborhood of the point A is shown in Fig. 9(a). (b): numerical (black) and analytical (gray) border collision bifurcation curves near the origin. (c): bifurcation diagram through the curve surrounding the origin in (b) parametrized by ϕ anti-clockwise. The gray regions indicate coexistence between two periodic orbits (d): periods of the detected orbits in (c).

one has

$$f_\ell f_r(0)(c_\ell, c_r) = c_\ell + 0.9(c_r - \pi) + O((c_r - \pi)^2)$$
$$(f_\ell f_r)'(0)(c_\ell, c_r) = 0.5 \cdot 0.9 + O((c_r - \pi)^2)$$

As the gap depends on lower order terms than the slope, it grows one order faster than the slope. Then, if c_r is close enough to π one can consider that the gap is varied while the slope remains constant. As mentioned in the introduction, this undergoes the so-called period adding big bang bifurcation and the orbits are organized by a Farey-tree-like structure. That is, near the big bang bifurcation, there exist an infinite number of bifurcation curves
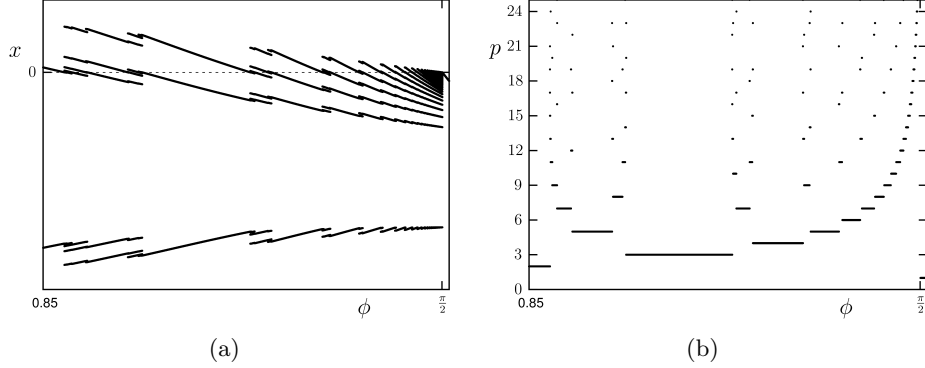
Figure 8: Bifurcation structure around the period adding big bang bifurcation ocuring at $(0, \pi)$ for Example 1. (a) Bifurcation diagram along the curve labeled in Fig. 7(a) and parametrized clockwise by ϕ . (b) Periods of the detected periodic orbits.

separating existence regions of different periodic orbits in such a way that, in between two regions there exists another region locating a unique periodic orbit obtained by "gluing" them and thus having a period which results from the addition of the periods of those. This implies that between two different bifurcation curves there exist an infinite number of them (see for example [4] for an extended explanation). This is shown in Fig. 8 by the one-dimensional bifurcation diagram along the curve shown in Fig. 7(a).

From the global overview of the bifurcation scenario shown in Fig. 7(a) it seems that all the bifurcation curves created at $(0, \pi)$ disappear at the intersection points of the curves $\xi^d_{\mathcal{RL}^n}$ and $\xi^c_{\mathcal{RL}^{n+1}}$. However, as we will immediately show, this can not be the case. Let us take a closer look for example at the point labeled with A in Fig. 7(a) as A whose surrounding is magnified in Fig. 9(a). As this point is given by the intersection of the curves $\xi^c_{\mathcal{RL}^2}$ and $\xi^d_{\mathcal{RL}}$, arguing as before, one can consider the map

$$
f_3(x) = \begin{cases} f_\ell f_r f_\ell(x) & \text{if } x \leq 0 \\ f_\ell f_r(x) & \text{if } x > 0 \end{cases}
\tag{13}
$$

and solve equations

$$
\begin{cases} f_\ell f_r f_\ell(0) = 0 \\ f_\ell f_r(0) = 0 \end{cases}
$$

to obtain the coordinates of A, which leads to $A = (c^A_\ell, c^A_r) \simeq (0.88325, 1.37759)$.

23

One could also consider the iterated function $f_r f_\ell f_\ell$ for the left branch. However, one can see that the first option is the proper way of writing the corresponding iterate, as it collapses the corresponding periodic orbit of (11) to the fixed point $x = 0$ of (13) at A.

Expanding the gaps and the slopes of each branch of $f_3(x)$ at the discontinuity in series of powers near A, one has

$$f_\ell f_r f_\ell(0)(\tilde{c}_\ell, \tilde{c}_r) \simeq 1.05483\tilde{c}_\ell + 0.17280\tilde{c}_r + O(\tilde{c}_\ell^2, c_r^2, \tilde{c}_\ell\tilde{c}_r) \tag{14}$$

$$(f_\ell f_r f_\ell)'(0)(\tilde{c}_\ell, \tilde{c}_r) \simeq 0.4935 \cdot 10^{-1} + 0.1994 \cdot 10^{-1}\tilde{c}_\ell + \tag{15}$$
$$0.25224\tilde{c}_r + O(\tilde{c}_\ell^2, \tilde{c}_r^2, \tilde{c}_\ell\tilde{c}_r)$$

$$f_\ell f_r(0)(\tilde{c}_\ell, \tilde{c}_r) \simeq \tilde{c}_\ell - 0.17280\tilde{c}_r + O(\tilde{c}_r^2) \tag{16}$$

$$(f_\ell f_r)'(0)(\tilde{c}_\ell, \tilde{c}_r) \simeq -0.86401 \cdot 10^{-1} + 0.44162\tilde{c}_r + O(\tilde{c}_r^2), \tag{17}$$

where $\tilde{c}_\ell = c_\ell - c_\ell^A$ and $\tilde{c}_r = c_r - c_r^A$. From Eqs. (14) and (16), it is clear that there exist two directions in the parameter space (presented in Fig. 9(a) as two dotted straight lines) along which the two gaps can be (locally) varied independently adding a positive offset at the left branch and a negative at the right one. As one can see from Eqs. (15) and (17), near the point A, $f_3(x)$ is of type increasing-decreasing. However, in that case, the slopes can not be decoupled from the offsets because they depend on the same order on the parameters c_ℓ and c_r. Nevertheless, we state that Theorem 2 remains valid as long as they do not change their sign and, therefore, there exists a big bang bifurcation of the period increment type at the point A. As the map undergoing the big bang bifurcation is the one defined in Eq. (13), the periodic orbits emerging at the point A are of type $\overline{\mathcal{RL}(\mathcal{RL}^2)^n}$. This is shown in Fig. 9(b) where a one-dimensional bifurcation diagram is performed along the corresponding segment labeled in Fig. 9(a). As the coexistence regions between the periodic orbits of type $\overline{\mathcal{RL}(\mathcal{RL}^2)^n}$ and $\overline{\mathcal{RL}(\mathcal{RL}^2)^{n+1}}$ can not be there observed, a magnification for the case $n = 2$ is shown in Fig. 9(c).

However, the question remains, where do all other border collision bifurcation curves created at $(0, \pi)$ end? As shown in Fig. 9(d), when moving away from A, there exists a point between the two segments labeled in Fig. 9(a) where the coexistence shown in Fig. 9(c) disappears. This point is given by the intersection of the corresponding curves $\xi^c_{\mathcal{RL}(\mathcal{RL}^2)^3}$ and $\xi^d_{\mathcal{RL}(\mathcal{RL}^2)^2}$ exactly as happened at the point A with the curves $\xi^c_{\mathcal{RL}^2}$ and $\xi^d_{\mathcal{RL}}$. Such a point would be the analagous to the given by the intersection of the curves $\xi^c_{\mathcal{RL}(\mathcal{RL}^2)}$ and $\xi^d_{\mathcal{RL}}$ labeled with B in Fig. 9(a). This self similarity suggests that this process takes place for every border collision curve, so

forming an infinite tree of big bang bifurcations of period increment type whose mother node is the point $(0,0)$, generating the complete period adding structure absorbed by the point $(0,\pi)$.

5.2   Example 2

Let us now consider a second example fulfilling conditions C.1–C.3

$$f(x) = \begin{cases} c_\ell + 0.4x(x+2) =: f_\ell(x) & \text{if } x \leq 0 \\ -c_r + 0.5x(x-1) =: f_r(x) & \text{if } x > 0 \end{cases} \tag{18}$$

which is shown in Fig. 10(a).

As expected, the origin of the parameter space $c_\ell \times c_r$, presented in Fig. 10(b), is a big bang bifurcation point of the period increment type. Moreover, arguing exactly as before, one can show that the situation between the points $(0,2)$ and $(0,0)$ is the same as in the previous example between $(0,\pi)$ and $(0,0)$. This has been validated with numerical simulations which we do not show as they are equivalent to the ones presented in Figs. 7(b), 7(c), 7(d) and 8. Therefore we omit further comments in that direction. However, there exists in the c_ℓ axis of Fig. 10(b) several points that deserve special interest. For example, let us consider the point $(1,0)$. One can easily see that the function

$$f_2(x) = \begin{cases} f_r f_\ell(x) & \text{if } x \leq 0 \\ f_r(x) & \text{if } x > 0 \end{cases} \tag{19}$$

is continuous at $(c_\ell, c_r) = (1,0)$ and, after re-parametrizing along proper directions in $c_\ell \times c_r{}^8$, fulfills conditions C.1–C.3. Therefore, the point $(1,0)$ represents a big bang bifurcation of period increment type where the orbits corresponding to the original map, f, are of type $\mathcal{R}(\mathcal{R}\mathcal{L})^n$. This is shown in Figs. 11(a) and 11(b) through the one-dimensional bifurcation diagram along the curve labeled in Fig. 10(b).

One can proceed analogously and show that the situation is repeated for the other points, $(p_n, 0)$, also located at the horizontal axis of Fig. 10(b). In order to show that, let us consider the equation

$$f_r^n f_\ell(0) = f_r(0), \; c_r = 0 \tag{20}$$

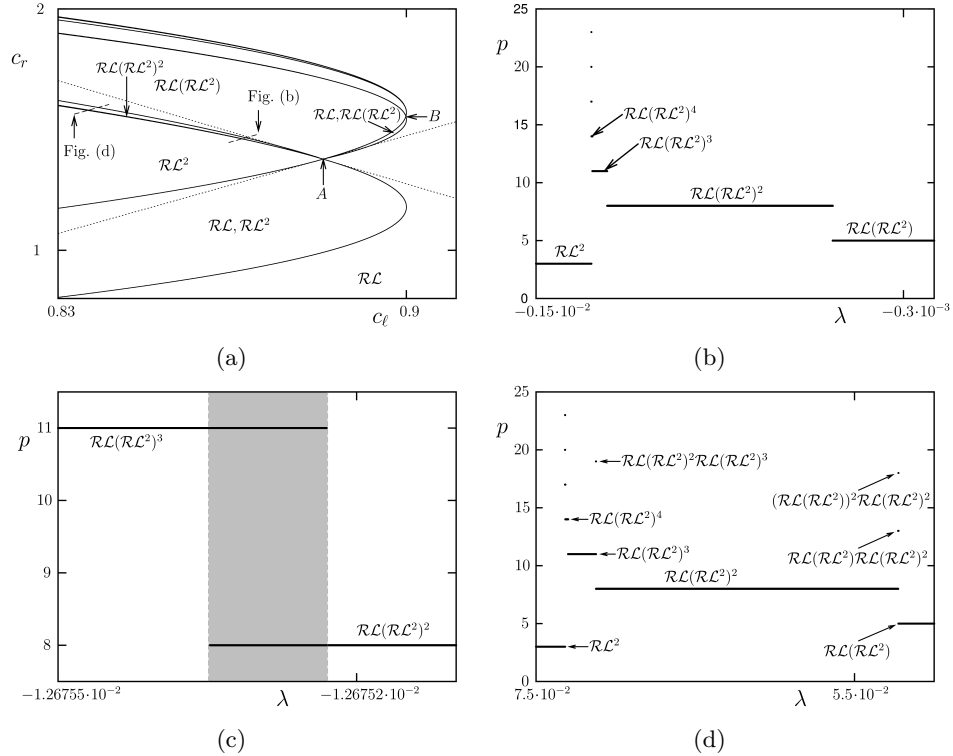[8]We skip the details as one has just to proceed as in Example 1.

Figure 9: Bifurcation scenario near the point A (see Fig. 7(a)). (a): Blow up labeled in Fig. 7(a). The two dotted straight lines are the directions along which the right and left images of 0 by $f_3(x)$ remain (locally) constant. (b): one-dimensional bifurcation diagram along the segment labeled in (a): period increment scenario. (c): maximization of the coexistence (gray region) between the periodic orbits $\mathcal{RL}(\mathcal{RL}^2)^2$ and $\mathcal{RL}(\mathcal{RL}^2)^3$. (d): bifurcation diagram along the segment labeled in (d); far enough from A, the period increment structure generated at A disappears.
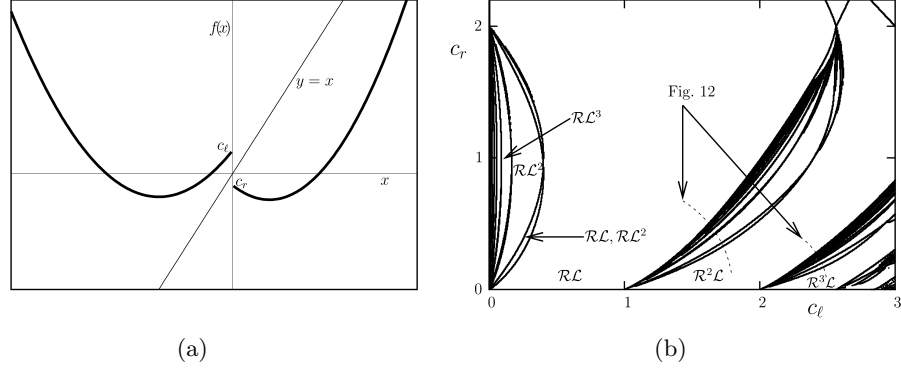
26

Figure 10: (a): system function of Example 2 defined in Eq. (18). (b): border collision bifurcation curves of Example 2.

and let p_n be the root of the Eq. (20) which is not a root of the same equation using $n-1$ instead of n. Then, one can easily see that the map

$$f_n(x) = \begin{cases} f_r^n f_\ell(x) & \text{if } x \leq 0 \\ f_r(x) & \text{if } x > 0 \end{cases} \tag{21}$$

is continuous at $(c_\ell, c_r) = (p_n, 0)$ and, again under proper re-parametrization, the conditions C.1–C.3 are hold at $(c_\ell, c_r) = (p_n, 0)$. Therefore, for every $(p_n, 0)$ there exists an open set containing that point such that only periodic orbits of type $\underline{\mathcal{R}(\mathcal{R}^n\mathcal{L})^m}$ exist for all m. Moreover, there exist regions in that open set where two $\underline{\mathcal{R}(\mathcal{R}^n\mathcal{L})^m}$ and $\underline{\mathcal{R}(\mathcal{R}^n\mathcal{L})^{m-1}}$ orbits coexist $\forall m$.

6 Conclusions

Big bang bifurcations occur in low-dimensional piecewise-smooth systems typically whenever two fixed points cross the boundary and become virtual. This is given by a transverse intersection between two border collision bifurcation curves when the considered parameters control the distance between the boundary and the fixed points.

So far we have presented this situation for the one-dimensional case for which the boundary is represented by a single point ($x = 0$) where the map has a
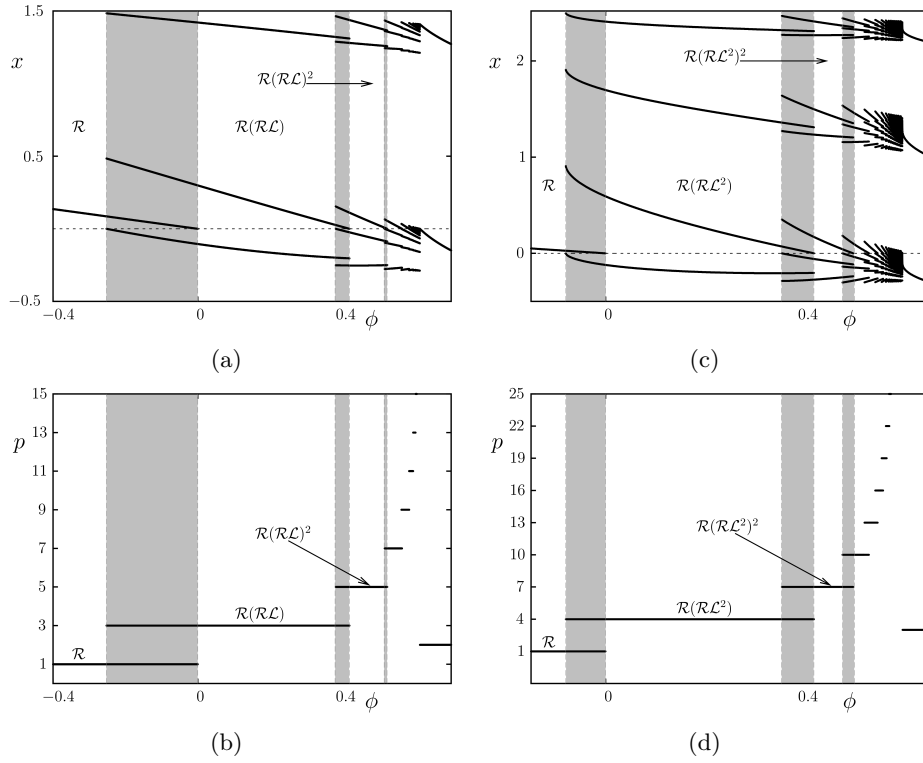
27

(a)

(c)

(b)

(d)

Figure 11: Bifurcation structure around the big bang bifurcation points at $(c_\ell, c_r) = (1, 0)$ ((a) and (b)) and $(c_\ell, c_r) = (p_2, 0)$ ((c) and (d)). (a) and (c) Bifurcation diagram along the curves labeled in Fig. 10(b). (b) and (d) periods of the periodic orbits. The gray regions indicate coexistence betwee two periodic orbits.

jump discontinuity. By Theorem 2, we have explicitly and rigorously characterized the infinite number of periodic orbits that appear after the collision of two fixed points with the boundary when the map is locally contractive and has eigenvalues of opposite sign: a big bang bifurcation of periodic increment type occurs. As mentioned in Remark 7, in the case that one of the slopes vanishes in an open set containing $x = 0$, the bifurcation scenario remains the same except that the coexistence regions disappear, and a big bang of the so-called pure increment type occurs.

We have also given examples showing that one can consider a proper renormalization of the map in order to study other big bang bifurcations in the parameter space. We have given evidence that the same result holds when allowing the eigenvalues of the linearization at the fixed points to vary with the parameters, although they should at least preserve their sign and the attracting condition. In the same examples we have also checked the result conjectured in the introduction; that is, when both eigenvalues are positive then the so-called period adding big bang bifurcation takes place. A proof of that we leave for future work. Using also renormalization arguments we have suggested that the bifurcation curves issuing from the detected period adding big bang bifurcation are "collected" by an infinite cascade of period increment big bang bifurcations. A rigorous and more detailed study of this situation will be reported elsewhere.

References

[1] Ll. Alsedà and A. Falcó, *On the topological dynamics and phase-locking renormalization of lorenz-like maps*, Ann. Inst. Fourier, 53 (2003), pp. 859–883.

[2] Ll. Alsedà and J. Llibre, *Kneading theory of lorenz maps*, Dynamical systems and ergodic theory, 23 (1989), pp. 83–89.

[3] Ll. Alsedà, J. Llibre, M. Misiurewicz, and C. Tresser, *Periods and entropy for lorenz-like maps*, Ann. Inst. Fourier (Grenoble), 39 (1989), pp. 929–952.

[4] V. Avrutin and M. Schanz, *On multi-parametric bifurcations in a scalar piecewise-linear map*, Nonlinearity, 19 (2006), pp. 531–552.

[5] V. Avrutin, M. Schanz, and S. Banerjee, *Multi-parametric bifurcations in a piecewise-linear discontinuous map*, Nonlinearity, 19 (2006), pp. 1875–1906.

[6] ——, *Codimension-3 bifurcations: Explanation of the complex 1-, 2- and 3D bifurcation structures in nonsmooth maps*, Phys. Rev. E, 75 (2007), pp. 1–7.

[7] P. C. COULLET, J. M. GAMBAUDO, AND C. TRESSER, *Une nouvelle bifurcation de codimension 2: le colage de cycles*, C. R. Acad. Sc. Paris, série I, 299 (1984), pp. 253–256.

[8] M. DI BERNARDO, C. J. BUDD, A. R. CHAMPNEYS, AND P. KOWAL-CZYK, *Piecewise-smooth Dynamical Systems: Theory and Applications*, vol. 163 of Applied Mathematical Sciences, Springer, 2008.

[9] J. GAMBAUDO AND C. TRESSER, *On the dynamics of quasi-contractions*, BOL. SOC. BRAS. MAT., 19 (1988), pp. 61–114.

[10] J. M. GAMBAUDO, P. GLENDINNING, AND C. TRESSER, *Collage de cycles et suites de Farey*, C. R. Acad. Sc. Paris, série I, 299 (1984), pp. 711–714.

[11] J. M. GAMBAUDO, P. GLENDINNING, AND T. TRESSER, *The gluing bifurcation: symbolic dynamics of the closed curves*, Nonlinearity, 1 (1988), pp. 203–14.

[12] J. M. GAMBAUDO, I. PROCACCIA, S. THOMAE, AND C. TRESSER, *New Universal Scenarios for the Onset of Chaos in Lorenz-Type Flows*, Phys. Rev. Lett, 57 (1986), pp. 925–928.

[13] R. GHRIST AND P. J. HOLMES, *Knotting within the gluing bifurcation*, in IUTAM Symposium on Nonlinearilty and Chaos in the Enginnering Dynamics, J. Thompson and S. Bishop, eds., John Wiley Press, 1994, pp. 299–315.

[14] P. GLENDINNING, *Topological conjugation of lorenz maps to β-transformations*, Math. Proc. Camb. Phil. Soc., 107 (1990), pp. 401–413.

[15] J. H. HUBBARD AND C. T. SPARROW, *The Classification of Topologically Expansive Lorenz Maps*, Communications of Pure and Applied Mathematics, XLIII (1990), pp. 431–443.

[16] R. LABARCA AND C. MOREIRA, *Bifurcation on the essential dynamics of lorenz maps and applications to lorenz-like flows: contributions to study of expanding case*, Bol. Soc. Bras. Mat., 32 (2001), pp. 107–44.

[17] ——, *Essential dynamics for lorenz maps on the real line and the lexicographical world*, Ann. I.H. Poincaré, AN 23 (2006).

[18] N. N. LEONOV, *Map of the line onto itself*, Radiofisika, 2 (1959), pp. 942–956. (in Russian).

[19] D.V. LYUBIMOV, A.S. PIKOVSKY, AND M.A. ZAKS, *Universal Scenarios of Transitions to Chaos via Homoclinic Bifurcations*, vol. 8 of Math. Phys. Rev., Harwood Academic, London, 1989. Russian version 1986 as a Preprint (192) of Russian Academy of Science, Institute of mechanics of solid matter, Sverdlovsk.

[20] C. MIRA, *Chaotic dynamics*, World Scientific, 1987.

[21] I. PROCACCIA, S. THOMAE, AND C. TRESSER, *First-return maps as a unified renormalization scheme for dynamical systems*, Phys. Rev. A, 35 (1987), pp. 1884–1900.

[22] C. SPARROW, *The Lorenz Equations*, Springer-Verlag, 1982.

[23] D. V. TURAEV AND L. P. SHIL'NIKOV, *On bifurcations of a homoclinic "figure of eight" for a saddle with a negative saddle value*, Soviet Math. Dokl., 34 (1987 (Russian version 1986)), pp. 397–401.